Journal of Environmental Chemical Engineering 10 (2022) 107024

Contents lists available at ScienceDirect

Journal of Environmental Chemical Engineering

journal homepage: www.elsevier.com/locate/jece

Enhanced adsorptive removal of carbendazim from water by $FeCl_3$-modified corn straw biochar as compared with pristine, HCl and NaOH modification

Yanru Wang [a], Jingbo Miao [a], Muhammad Saleem [b], Yong Yang [a], Qingming Zhang [a,*]

[a] Key Lab of Integrated Crop Pest Management of Shandong Province, College of Plant Health and Medicine, Qingdao Agricultural University, Qingdao, Shandong 266109, China
[b] Department of Biological Sciences, Alabama State University, Montgomery, AL 36101, USA

ARTICLE INFO

Editor: Despo Kassinos

Keywords:
Corn straw biochar
Fungicides
Modification
Removal mechanisms
Pyrolysis temperature

ABSTRACT

Carbendazim residues were widely present in the worldwide water which caused a potential risk to water ecosystem and human health. Therefore, it is necessary to develop environmentally friendly ways to eliminate its residue in the contaminated water environments. Herein, the corn straw biochars were prepared at 300 (BC300), 500 (BC500), and 700 °C (BC700). Moreover, using BC700 as precursor, three novel adsorbents of acid, alkali, and iron magnetization modified biochar (named as BC700H, BC700N, and BC700M, respectively) were synthesized to adsorptive removal of carbendazim from water. Results showed that the adsorption capacity of six biochar materials for carbendazim was in the following order BC700M>BC700H>BC700N>BC700 >BC500 >BC300. The maximum adsorption amount of BC700M reached up to 108.1 mg g^{-1}. The adsorption of carbendazim was a spontaneous, endothermic, and randomly increasing process, while both physisorption and chemisorption were involved in adsorption process for all prepared biochar materials. For BC700M, pore filling, π-π interaction, oxygen-containing groups, and Fe-O complexation were main mechanisms. The BC700M can be easily separated and regenerated at least five times under a wide pH range. Overall, as compared to the other five biochar materials, this study indicates that Fe-modified corn straw biochar is a promising and sustainable adsorbent for carbendazim removal from water environment.

1. Introduction

Carbendazim (methyl-2-benzimidazolecarbamate) is an extensively used fungicide to control plant diseases in agricultural field [1]. Because of its negative effects on human health and other non-target organisms even at low concentrations, carbendazim has been banned in some countries such as USA and Australia. However, it is still permitted to be produced and used in various formulations in some developed and developing countries such as Portugal, China, Brazil and India [1–3]. Carbendazim is chemically stable and relatively persistent with the half-lives ranged from several days to hundreds of days in different environments [4–6]. In addition, carbendazim is also the hydrolytic product of fungicides thiophanate methyl and benomyl in natural conditions [7]. The frequent application of carbendazim and other benzimidazole fungicide results in its accumulation in soil and water environments [8]. Previous studies have reported that different concentrations of carbendazim (0.003 μg L^{-1}-156 μg L^{-1}) have been detected in various water environments including surface water [9], groundwater [10], sea water [11], municipal sewage [12], and even drinking water [13]. Thus, effective and eco-friendly removal of this fungicide from water-bodies is very essential for protection of water resources for human use and other living organisms.

Up to now, many removal methods such as adsorption [14], biological degradation [15], advanced oxidation [8], and photocatalytic treatments [16] have been suggested to treat carbendazim contaminated water and soil environments. Among the removal techniques, adsorption is regarded as one of the safest and most effective method to remove pollutants from water owing to cheaper, simple, and easy availability of materials used for adsorption [17]. Biochar is a stable and porous carbon material, which is also regarded as an environment-friendly adsorbent. In recent years, biochar has been widely used in wastewater treatment because it has many unique characteristics including low cost,

* Corresponding author.
E-mail address: qmzhang@qau.edu.cn (Q. Zhang).

https://doi.org/10.1016/j.jece.2021.107024
Received 17 October 2021; Received in revised form 10 December 2021; Accepted 15 December 2021
Available online 17 December 2021

readily-availability, high-efficiency, and environment-friendly properties [17–19]. Usually, adsorption capacity is the most important indicator of biochar quality for removing pollutants, which can be influenced by biomass type, carbonization condition, and chemical modification [20,21] Chemical modification methods include but are not limited to these: acid-and alkali-modification and doping certain elements (e.g., P, S, Fe, and Zn etc.) to improve the biochar surface structure and or endow special functional groups for enhancing the biochar adsorption capacity [22–25]. Using biochar as adsorbent to remove carbendazim from water and soil environments has also been reported in recent years. For example, Ding et al. [26] prepared sewage sludge derived biochar under pyrolysis temperatures of 100–700 °C and found that 700 °C pyrolyzed biochar possessed maximum removal efficiency of carbendazim from soil environment. Wang et al. [27] prepared rape straw derived biochar that was treated with H_3PO_4 at 300–600 °C, and they found higher temperature pyrolyzed and P doped biochar have better adsorption capacity to remove carbendazim from the water environments. However, there is a need for biochar produced from various biomass resources to improve removal process of carbendazim from contaminated environments. Moreover, the recovery of used biochar powder from the treated water is also a big problem. These issues highlight the need for further studies on how to improve the properties of biochar for increasing its adsorption capacity of carbendazim and facilely separated after use.

Corn straw as an abundant natural material in China is usually discarded or burned resulting in environment pollution [23]. It is very necessary to reasonable unitization of this corn waste for eco-environmental sustainability. Therefore, in this study, we used corn straw as raw material to prepare biochar under three pyrolysis temperatures (300, 500, and 700 °C). Moreover, the acid-, alkali-, and Fe-modified biochar were prepared using raw biochar as precursor through a one-step method. The adsorption capacity of the prepared biochar for carbendazim from aqueous solutions was determined and compared for selecting the best adsorbent. The physical and chemical characteristics of the prepared biochar were analyzed. A series of experiment were conducted to investigate the adsorption kinetics, thermodynamics, affect factors, and adsorption mechanisms of carbendazim adsorption by prepared biochar material. The objective of this study is to provide an efficient material for highly efficient removal of carbendazim from water environment.

2. Materials and methods

2.1. Chemicals and preparation of biochar and modified biochar

Fungicide carbendazim (purity, 97%) was supplied by Hailir Pesticides and Chemicals Group (Qingdao, China). Stock solution of carbendazim (300 mg L^{-1}) was prepared in methanol for gradient dilution to construct quantitative standard curve. Methanol (HPLC grade) was purchased from Sigma-Aldrich (St. Louis, MO, USA). Other analytical reagents such as HCl, NaOH, and $FeCl_3$ were purchased from commercial corporations.

Corn straw (*Zea mays* L.) was collected from Crop Garden of Qingdao Agricultural University, China. The collected corn straw was first thoroughly washed with distilled water to remove water soluble impurities and surface adhered particles and then dried at 85 °C overnight until a constant weight of the material was obtained. The dry biomass was then crushed and sieved into a particle size of less than 0.6 mm for biochar preparation. The feedstock was placed into a tube furnace and pyrolyzed at 300, 500, and 700 °C for 2 h under continuous N_2 environment, and then it was washed with distilled water to neutrality, and dried at 85 °C. The biochar produced at 300, 500, and 700 °C were named as BC300, BC500, and BC700, respectively. As for acid- and alkali- modification, BC700 was soaked in 1 M HCl and NaOH solutions, respectively, stirred and reacted at room temperature (25 ± 2 °C) for 24 h, then washed with distilled water to neutrality, and dried at 85 °C [28]. The obtained acid- and alkali- modification biochars were named as BC700H and BC700N, respectively. As for magnetic biochar, 10 g corn straw powder was soaked in 100 mL of 1 M $FeCl_3$ solution and continuously stirred for 24 h at room temperature, then centrifuged at 5500 rpm for 15 min to remove supernatant, followed by drying at 85 °C for 24 h [29]. The dried samples were placed into a tube furnace and pyrolyzed at 700 °C for 2 h under continuous N_2 environment, then washed with distilled water to neutrality, and dried at 85 °C. The obtained Fe-modified biochar was named as BC700M. All the prepared biochar materials were put into sealed bags before use.

2.2. Characterization of biochar materials

Total carbon (C), hydrogen (H), oxygen (O), and nitrogen (N) contents of samples were determined by an elemental analyzer (Elemantar Vario EL cube, Germany). The specific surface area and pore size distribution of samples were measured by an automatic specific surface and porosity tester (Belsorp- Mini II, Japan). The morphology of the samples was observed using a scanning electron microscopy (SEM, Zeiss Gemini300, Germany). In addition, a transmission electron microscope (JEM-2100 F, Joel, Japan) was used to observe the morphology of the Fe-modified biochar. The surface functional groups of the samples were analyzed via a Fourier transform infrared spectroscopy (FTIR, Bruker Vertex 70, Germany). The surface crystallinity of Fe-modified biochar was characterized by an X-ray diffractometry (XRD, Bruker D8 Focus, Germany).

2.3. Adsorption experiments

All the adsorption experiments of carbendazim on various biochar materials were performed in a batch mode. Each treatment was conducted in triplicates. For the adsorption kinetic studies, 10 mg of biochar materials were weighed into carbendazim aqueous solution (30 mL, 25 mg L^{-1}) and stirred at 150 rpm at room temperature. Aliquots (1.0 mL) were sampled at 0, 0.17, 0.33, 0.5, 0.75, 1.0, 1.5, 2.5, 5, 9, 14, and 24 h, filtered through 0.45 μm filters for determination of carbendazim concentration. For the adsorption thermodynamics studies, 10 mg of biochar materials were put into a series of concentrations (5.0, 10.0, 15.0, 20.0 and 30.0 mg L^{-1}) of carbendazim aqueous solution (30 mL) and stirred at 150 rpm at 25, 35, and 45 °C. After equilibrium, the concentration of carbendazim in supernatant was determined. Finally, the effects of pH on adsorption of carbendazim were also studied. The experimental protocol is same with thermodynamics experiment. The concentration of carbendazim in supernatant were determined by ultra-high performance liquid chromatography (UHPLC, Thermo Scientific Vanquish, USA) equipped with a reversed-phase C18 column (Thermo Hypersil GOLD, 3 μm, 2.1 mm × 100 mm) and a UV detector at a wavelength of 281 nm. The mobile phase was consisted of methanol and water (50:50, v/v) with a flowrate of 0.3 mL min^{-1}.

2.4. Data analysis

All treatments of adsorption experiment were in triplicate and the data were presented as mean ± standard deviation (SD) at confidence intervals of 95%. The calculation equations of adsorption amount, and kinetic, isotherm and thermodynamic models were provided in Text S1 of Supplementary Information.

3. Results and discussion

3.1. Characterization of the biochar materials

The element (C, H, O, and N) composition, specific surface area, and pore size distribution of biochar materials are given in Table 1. For non-modified corn straw biochar, with the increasing of pyrolysis temperatures, the C contents obviously increased, while the H and O contents

Table 1
The physio-chemical properties of biochar materials.

Adsorbents	Composition (%)				Atomic ratio			Surface area (m^2 g^{-1})	Pore volume (cm^3 g^{-1})
	C	H	O	N	H/C	O/C	(O+N)/C		
BC300	56.57	4.69	20.47	1.27	0.99	0.27	0.29	4.35	0.03
BC500	64.01	2.54	15.23	1.12	0.48	0.18	0.19	7.91	0.05
BC700	70.76	1.65	9.42	1.03	0.28	0.10	0.11	33.3	0.08
BC700H	73.56	1.38	8.41	1.06	0.23	0.09	0.10	40.24	0.13
BC700N	72.15	1.24	8.52	1.12	0.21	0.09	0.10	82.64	0.17
BC700M	71.48	1.58	9.37	1.02	0.27	0.10	0.11	173.9	0.33

obviously decreased, and the N content was relatively steady although has a slight decrease. This can be attributed to the fact that higher pyrolysis temperature resulted in the loss of H and O, thereby leading to the accumulation of C contents [30]. The elemental ratios of H/C, O/C, and (O+N)/C are usually used to indicate the carbonization, aromaticity, and polarity, respectively [31]. According to the changes in the values of these indicators (Table 1), the aromaticity of biochar was increased, and it was accompanied by a decrease in polarity with the pyrolysis temperature increasement. As for modified biochar materials, the values of elemental composition and ratios for BC700H, BC700N, and BC700M were similar to those of BC700. These results indicated that HCl, NaOH, and $FeCl_3$ modification did not produce obvious effects on the chemical characteristics of the corn straw biochar. The larger surface areas and pore volumes of corn straw biochar were observed with pyrolysis temperature increasement. This is because the pores are not well formed in plant tissues at low temperature. With increasing of pyrolysis temperature, aliphatic and volatile ingredients were removed and the amorphous carbons condensed to crystalline carbons which was conducive to the formation of more pores [32,33]. After biochar treatment with HCl, NaOH, and $FeCl_3$, the surface areas were increased from 33.3 m^2 g^{-1} to 40.24, 82.64, and 173.9 m^2 g^{-1}, respectively (Table 1), indicating that acid- and alkali-, especially iron modification could significantly increase the specific surface area and pore volume of the biochar [17,22].

The SEM observation demonstrated that the surface of corn straw biochars produced at three pyrolysis temperatures were smooth and have multiple different sizes of pores (Fig. 1a, b, and c). However, after being treated by HCl and NaOH, the surface of the biochar materials became rough and partial collapse and more small pores were observed (Fig. 1d and e), indicating that chemical modification using HCl and NaOH might corrode the raw biochar and change its surface morphology [20]. When the biochar was modified by $FeCl_3$, the surface of the biochar changed much rougher and many irregular particles adhered to the surface of biochar (Fig. 1f), indicating that Fe was successfully impregnated in the surface and in the pore structure of biochar. The TEM image of Fe-modified biochar further exhibited that the rod-shaped iron oxide crystals were deposited on the surface of the biochar (Fig. 2), which was also confirmed by the results of XRD. This can be attributed that $FeCl_3$ could react with carbohydrate polymers on the biochar

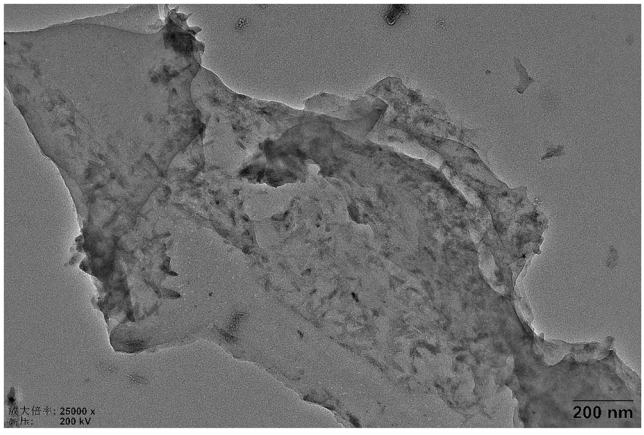

Fig. 2. TEM image of $FeCl_3$ modified biochar.

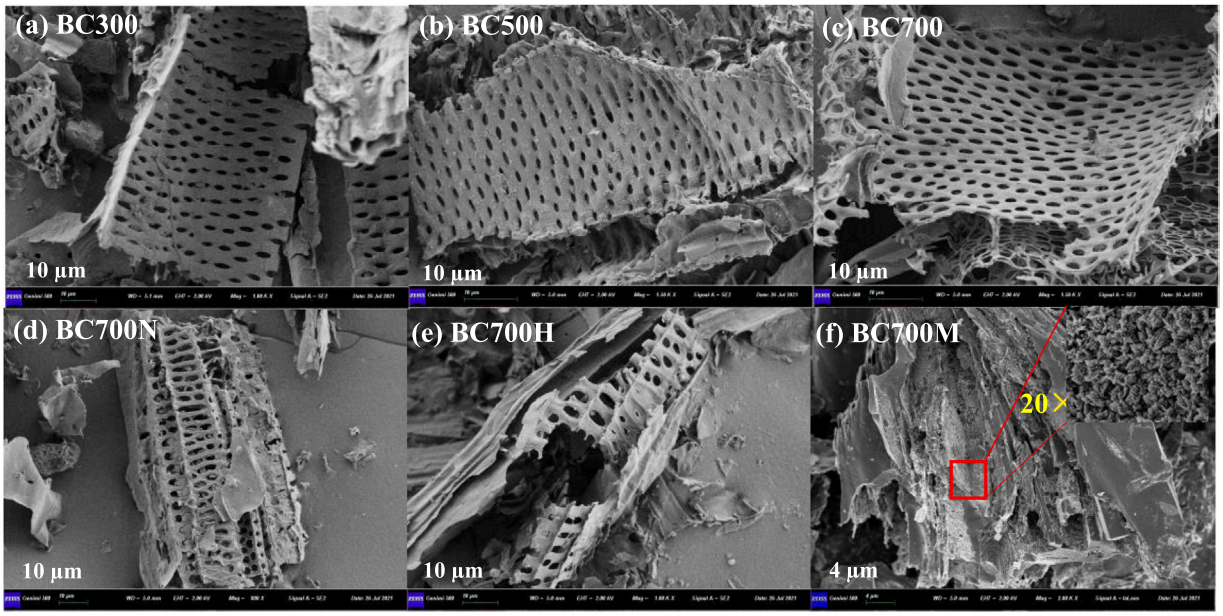

Fig. 1. SEM images of biochar materials.

surface during the pyrolysis process, causing the formation of bulk particles and decomposition of biochar surface, which implies that the adsorption sites and ion exchanged capacity of biochar improved [17, 34].

The XRD spectra of prepared biochar materials are illustrated in Fig. 3a. As for the non-modified corn straw biochar, the wide diffraction peaks near 2θ= 22° were the characteristic peaks of cellulose and hemicellulose [35]. With increasing of pyrolysis temperature, the intensities of the characteristic peaks were gradually decreased. This could be attributed to the fact that higher temperature causes the destruction of cellulose microcrystalline structure and the release of volatile components [35]. In BC500 and BC700, the presence of sylvite mineral (2θ=28.3° and 40.8°), quartz (2θ=26.7°), and calcite (2θ=49.1°) were observed, indicating that the crystallinity of minerals was formed at higher pyrolysis temperature [36]. Except for peaks of sylvite mineral, the XRD spectra of BC700N and BC700H were similar to that of BC700, indicating that HCl and NaOH treatments have little effect on the overall crystal structure of biochar. However, $FeCl_3$ treatment (BC700M) significantly changed the XRD spectra of biochar. Obvious diffraction peaks of Fe_3O_4 (2θ=30.2°, 43.1°, 57.1°, and 62.6°) and γ-Fe_2O_3 (2θ=35.5°) were observed [37]. It was confirmed that biochar surface had large amount of iron oxides, which was in good agreement with the results of the SEM and TEM analysis.

The FTIR spectra of prepared biochar materials are shown in Fig. 3b. The broad peak near 3400 cm^{-1} corresponded to the -OH stretch vibration. At 300, 500, and 700 °C (BC300, BC500, and BC700), its intensity decreased with increasing temperature, which indicated that higher temperature promoted the dehydration of cellulose and ligneous compounds [38]. The peak near 2918 cm^{-1} corresponded to the vibration of long-chain aliphatic carbon. Its intensity gradually decreased with increasement of pyrolysis temperature, thus implying that aliphatic carbon was destroyed at higher temperatures [39]. The peaks at 800–1700 cm^{-1} were regarded as the vibration of some aromatic functional groups such as C═C, C═O, and C-OH, etc. [40]. Their intensities were decreased with increasing of pyrolysis temperature suggesting that higher temperature increased the aromaticity of corn straw biochar [30]. As compared to BC700, the infrared peaks of samples BC700N and BC700H did not change obviously except for the intensity, indicating that NaOH and HCl modification could not change the types of functional groups but they changed the number of some functional groups. The peak intensity of -OH increased after acid-base modification as compared to the non-modification indicating that the oxygen-containing functional groups increased on the biochar surface. These oxygen-containing groups on the biochar could enhance the adsorption of biochar on organic substances by providing certain active sites [22]. As for $FeCl_3$ modification (BC700M), the infrared spectrum was similar to that of unmodified biochar (BC700), indicating that Fe particles have little effect on the types of functional groups in biochar. However, the peak near 557 cm^{-1} corresponded to the vibration of Fe-O bond [41]. Compared with the modified biochar, this peak gets wider and weaker in Fe-modified biochar, indicating that iron oxide particles were successfully loaded onto the surface of biochar [42,43]. This result was also confirmed via TEM and XRD.

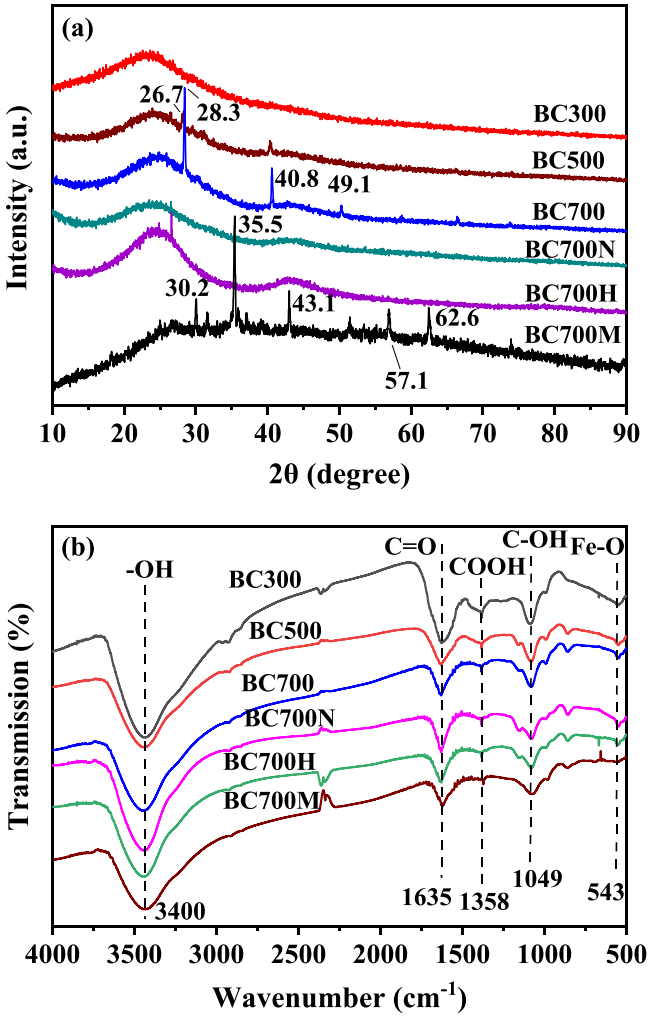

Fig. 3. XRD patterns (a) and FTIR spectra (b) of biochar materials.

3.2. *Adsorption kinetics of carbendazim onto biochar materials*

Overall, the adsorption of carbendazim onto biochar materials exhibited an initially rapid process followed by a slow process until an equilibrium was reached. As shown in Fig. 4a, the maximum adsorption quantities of prepared biochar materials for carbendazim were in the order BC700M (108.1 mg g^{-1})>BC700H (63.2 mg g^{-1})>BC700N (61.6 mg g^{-1})>BC700 (49.5 mg g^{-1})>BC500 (30.7 mg g^{-1})>BC300 (23.5 mg g^{-1}), indicating that Fe-modified biochar was the best adsorbent for removal of carbendazim from aqueous solution. Moreover, our results also indicated that the adsorption quantities of unmodified biochar increased with increasing pyrolysis temperature. According to the physicochemical characteristic of prepared biochar, the higher adsorption quantity can be attributed to the formation of higher pore structures, specific surface area, and functional groups [20,29,44]. Biochar materials BC700, BC700N, BC700H, and BC700M were selected as the adsorbent in the next series of experiment due to their higher carbendazim removal efficiencies. To clarify the adsorption process, herein, the pseudo first-order and pseudo-second-order models were firstly used to analyze the adsorption kinetics of carbendazim (Fig. 4b and c, Table S1). It was shown that, for four biochar materials, the calculated correlation coefficient (R^2) values by pseudo-second-order model were above 0.90 and higher than the R^2 values calculated by pseudo first-order model. Moreover, the calculated adsorption quantities (q_e) by pseudo-second-order model were better fitted with the experimental data. Therefore, the adsorption process of carbendazim was well described by a pseudo-second-order model, indicating the adsorption process was affected by chemical interactions [27]. The more detailed carbendazim adsorption onto the four biochar materials was obtained by an intra-particle diffusion model (Fig. 4d, Table S2). The result showed that adsorption process includes two sequential processes. The first stage was the instantaneous adsorption of carbendazim onto the external surface of the biochar materials, indicating that the diffusion rate of boundary layer was faster than that of intra-particle diffusion [23]. The second stage was the carbendazim molecules entered into the pores of biochar material and finally reached an equilibrium state, which was a gradual adsorption controlled by the intraparticle adsorption and diffusion process. This can be attributed to the extremely low

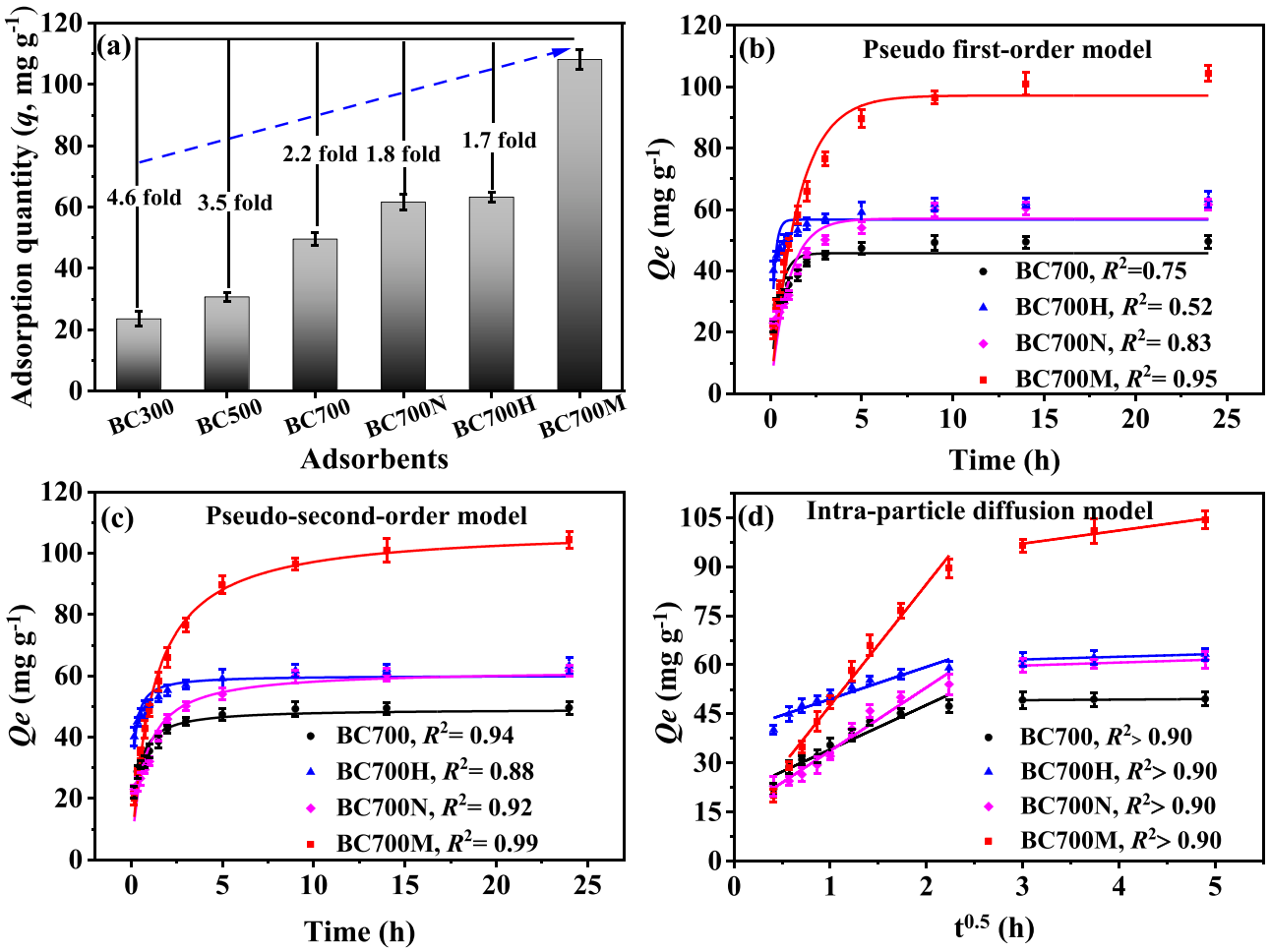

Fig. 4. The maximum adsorption quantity of carbendazim onto biochar materials (a); pseudo-first-order kinetic model fitting curves (b); pseudo-second-order kinetic model fitting curves; intra-particle diffusion model fitting curves (d).

carbendazim concentration left in the water and limited adsorption sites of the adsorbent surface [27,45]. In addition, the constants (*c*) were not zero, which indicated that the intra-particle diffusion was not the only rate-limiting step in the adsorption process and other adsorption mechanisms could also affect the adsorption process of carbendazim in some degree [46].

3.3. Adsorption isotherms of carbendazim onto biochar materials

The adsorption behaviors of carbendazim onto four biochar materials were examined by Langmuir and Freundlich isotherm models (Fig. 5), and the calculated parameters are given in Table S3. As for BC700, BC700H, and BC700N, the R^2 values are 0.976, 0.952, and 0.913 for Langmuir isotherm model, and 0.970, 0.927, and 0.902 for Freundlich isotherm model, respectively. This suggested that both isotherm models could well describe the adsorption isotherm effect, and the mono- and multiple-layer adsorptions played an important role in removing carbendazim from water by BC700, BC700H, and BC700N. However, for BC700M, Freundlich isotherm model (R^2 =0.946) fitted the data well than Langmuir isotherm model (R^2 =0.804), thus indicating that the multilayer adsorption was the main way to remove carbendazim toward the heterogeneous surface of the Fe-modified biochar [14]. In addition, the K_L value (0.869, calculated by Langmuir isotherm model) for BC700M was higher than those of other biochar materials and the 1/n value (0.321, calculated by Freundlich isotherm model) for BC700M was the smallest in all four biochar materials. This further indicated that Fe-modified biochar had the strongest adsorption affinity

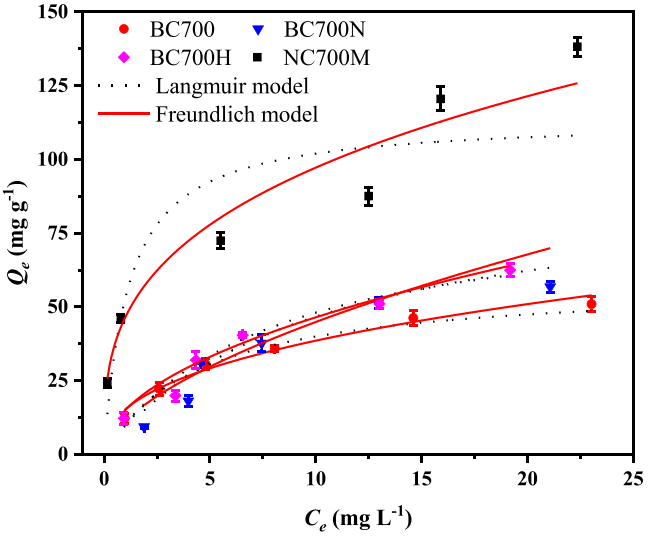

Fig. 5. Isotherm fitting curves of carbendazim adsorption onto biochar materials.

towards carbendazim as compared to the other biochar materials [47].

3.4. Adsorption thermodynamics of carbendazim onto biochar materials

The thermodynamic parameters such as Gibbs free energy change (ΔG°), enthalpy change (ΔH°) and entropy change (ΔS°) are usually used to analyze the adsorption mechanism [28,46,48]. In this study, as shown in Table 2, the values of ΔG° were negative for all adsorbents, suggesting that adsorption process was spontaneous [49]. Moreover, the ΔG° value was in the range of −20–0 kJ mol^{-1}, indicating that the adsorption of carbendazim onto BC700, BC700H, BC700N, and BC700M was primarily a physical adsorption process [48]. The ΔH° values of all the treatments were positive, demonstrating that the carbendazim adsorption was an endothermic process and a relatively high temperature is more favorable [50]. This result was also confirmed by the effect of temperature on carbendazim removal (Fig. S1). The values of ΔS° were positive for all the prepared biochar materials, indicating that the randomness at the solid-solution interface increased during adsorption process due to the desolvation of carbendazim molecule impregnated the adsorbents surface [51,52]. In this study, particularly, Fe-modified biochar (BC700M) displayed the greater randomness, which also supported its better adsorption performance [53].

3.5. Influence of initial pH

The adsorption characteristics of carbendazim on to four biochar materials under different pH ranges are shown in Fig. 6a. The adsorption of carbendazim initially increase (pH<5) and then deceased at higher pH (pH>8). Under pH range of 5–8, the higher adsorption capacity and a steady state were observed for each biochar materials, indicating that the prepared biochar materials could be used to effectively remove carbendazim from water with a wide pH range [27]. Carbendazim is an ionic organic compound with dissociation constant of pK_{a1}= 4.2 and pK_{a2}= 9.6 [54]. Thus, it exists as a cation form at pH < 4.2, and as anion form at pH> 9.6, while it is in a neutral molecule form when 4.2 < pH < 9.6 [14]. The zeta potential of BC700, BC700H, BC700N, and BC700M decreased with pH increment and their zero potential charge (pH_{zpc}) were 4.28, 4.13, 4.48, and 4.65, respectively (Fig. 6b). Generally, the adsorbent surface has positive charge when the pH of solution is below its pH_{zpc}, otherwise it has negative charge [55]. Therefore, the adsorption capacities of four biochar materials obvious decreased in acid and alkaline solutions and it was attributed to the greater electrostatic repulsion [56]. In near neutral environment, carbendazim exists as a neutral molecule without charge, the adsorption is independent of the electrostatic interaction. This environment is conducive to other adsorption effects (e.g., pore-filling, hydrophobic interactions, H-bonding, and π-π interaction) that improve the adsorption efficiency [27].

Table 2
Thermodynamic parameters of carbendazim adsorption onto four biochar materials.

Adsorbents	Temperature (K)	ΔG° (kJ mol^{-1})	ΔH° (kJ mol^{-1})	ΔS° (J mol^{-1} K^{-1})
BC700	298	-13.67	7.66	51.34
	308	-14.16		
	318	-15.33		
BC700H	298	-12.90	10.18	77.48
	308	-13.66		
	318	-14.48		
BC700N	298	-8.16	9.83	64.39
	308	-9.90		
	318	-11.07		
BC700M	298	-12.21	11.22	88.92
	308	-12.87		
	318	-13.46		

3.6. Regeneration and application of Fe-modified biochar

Our results showed the adsorption capacity of Fe-modified biochar (BC700M) for carbendazim was the highest in all prepared biochar materials. Its adsorption capacity was 2.2, 1.8, and 1.7 times than that of BC700, BC700N, and BC700H, respectively (Fig. 4a). Compared with previously reported adsorbents (Table S4), BC700M had comparable or higher adsorption capacity, suggesting the application potential for pollutants removal from aquatic environments. In addition, Fe-modified biochar was more conducive to recycling and reuse. Therefore, herein, the regeneration of BC700M was investigated. According to the preliminary experiment, 1.0 M HCl was used as the desorption solvent because it has the most desorption efficiency (>95.0%). The regeneration was performed with 10 mg BC700M with 30 mL carbendazim solution (25 mg L^{-1}). Result showed that adsorption capacity of BC700M on carbendazim slightly decreased with increasing number of cyclic utilization (Fig. 6c), which may be attributed to the fewer active sites caused by incomplete desorption of carbendazim onto BC700M surface. However, after five rounds of recycling, the carbendazim removal efficiency of BC700M was still above 85% (Fig. 6c), suggesting that $FeCl_3$ modified corn straw biochar is an excellent and reusable absorbent material for carbendazim removal from aquatic environment. To further clarify the applicability of the BC700M, a simple adsorption experiment for the removal of carbendazim from actual waterbodies was performed. The obtained removal rates of carbendazim were 98.7% and 96.8% from tap water and river water, respectively. This result indicated that $FeCl_3$ modified corn straw biochar could effectively remove carbendazim from the actual water environment.

3.7. Possible mechanism of carbendazim adsorption

In this study, the above characterization analysis, adsorption kinetics, isotherms, thermodynamics, and pH experiment revealed that multi-mechanisms including physisorption and chemisorption played crucial roles in carbendazim adsorption onto the prepared biochar materials. Physio-chemical properties illustrated that higher pyrolysis temperature and modification significantly increased specific surface area of biochar, which positively related to the carbendazim adsorption amount. This indicated that pore-filing was a main factor determining the carbendazim adsorption. Pseudo-second-order model well described the adsorption process, indicating that hydrogen bonding and π-π conjugation were involved in the adsorption process [55]. Moreover, intraparticle diffusion was regarded as the important rate-limiting step which was allocated to the microporous of biochar. Fitting results from isotherm models indicated that monolayer chemisorption and multilayer physisorption were formed on the prepared biochar materials [17]. The values of ΔH°,ΔG° and ΔS° suggested that $FeCl_3$-modified biochar had the greater spontaneity and randomness in carbendazim adsorption process [24]. As for BC700M, FTIR result illustrated the new peak at 1157 cm^{-1} appeared after adsorption (Fig. S2a), indicating that some forces such as hydrogen bounds, π-π interactions, and van der Waals forces played important roles in conjugation between carbendazim and the oxygen-containing functional groups of biochar [25,57]. Moreover, the XRD spectra has not obvious difference before and after adsorption (Fig S2b), implying that the Fe-O structural compounds provided more available active sites and enhanced the adsorption of carbendazim by surface complexation [17]. Overall, the mechanisms of carbendazim onto four biochar materials, especially Fe-modified biochar, were dominated by pore filling, π-π interaction, oxygen-containing groups, and Fe-O complexation.

4. Conclusions

In this study, six corn straw derived biochar materials were successfully prepared and tested for their ability to remove carbendazim from water environment. The results showed that pyrolysis temperature

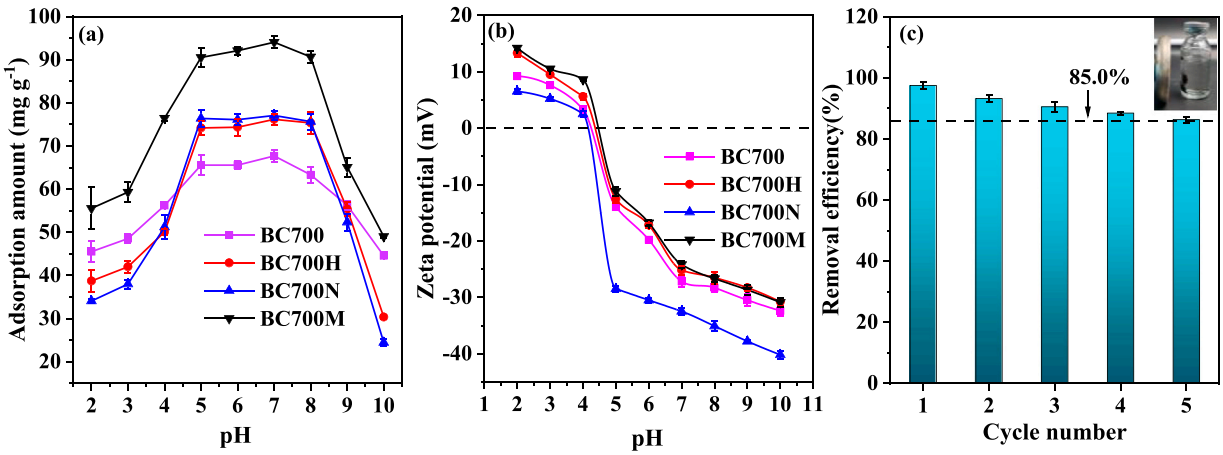

Fig. 6. Adsorption capacity of carbendazim onto biochar materials at different pH(a); zeta potential of adsorbents (b); adsorption capacity of BC700M over five cycles of regeneration.

had a positive effect on increasing biochar surface area, pore structure and functional groups, all these properties accelerated the adsorption of carbendazim. Pristine biochar was modified by HCl and NaOH, especially $FeCl_3$ at 700 °C significantly increased the adsorption of carbendazim in a near neutral solution (pH 5–8). The maximum adsorption capacity of Fe-modified biochar (BC700M) onto carbendazim reached up to 108.1 mg g^{-1}. The pseudo-second-order kinetic model and Freundlich isotherm model fitted well with experimental data. The adsorption of carbendazim was a spontaneous, endothermic, and randomly increasing process. The adsorption of carbendazim onto BC700M were dominated by physical and chemical mechanisms. The main adsorption mechanisms included pore filling, π-π interaction, oxygen-containing groups, and Fe-O complexation. Additionally, BC700M can be effectively regenerated and applied in the actual carbendazim contaminated water, indicating that $FeCl_3$ modified corn straw biochar was a promising and sustainable adsorbent for purification of water environment contaminated by organic pollutants.

CRediT authorship contribution statement

Yanru Wang performed experiment, analyzed data, and wrote original draft. **Jingbo Miao** performed materials Characterization. **Muhammad Saleem** reviewed and revised the manuscript. **Yong Yang** analyzed experimental data. **Qingming Zhang** designed the experiment, supplied funding, and edited the manuscript. All authors read and approved the final manuscript.

Declaration of Competing Interest

The authors declare that they have no known competing financial interests or personal relationships that could have appeared to influence the work reported in this paper.

Acknowledgements

This work was supported from Graduate Innovation Program Project of Qingdao Agricultural University (QNYCX21045) and Primary Research & Development Plan of Shandong Province, China (2017GSF21112).MS gratefully acknowledges funding from National Science Foundation (NSF-USA) under award 2100777.

Appendix A. Supporting information

Supplementary data associated with this article can be found in the online version at doi:10.1016/j.jece.2021.107024.

References

[1] S. Singh, N. Singh, V. Kumar, S. Datta, A.B. Wani, D. Singh, K. Singh, J. Singh, Toxicity, monitoring and biodegradation of the fungicide carbendazim, Environ. Chem. Lett. 14 (2016) 317–329.
[2] T. Ding, W. Li, J. Li, Toxicity and metabolic fate of the fungicide carbendazim in the typical freshwater diatom navicula species, J. Agric. Food Chem. 67 (2019) 6683–6690.
[3] Z. Huan, J. Luo, Z. Xu, D. Xie, Acute toxicity and genotoxicity of carbendazim, Main impurities and metabolite to earthworms (*Eisenia foetida*), Bull. Environ. Contam. Toxicol. 96 (2016) 62–69.
[4] P.J. Van den Brink, J. Hattink, F. Bransen, E. Van Donk, T.C.M. Brock, Impact of the fungicide carbendazim in freshwater microcosms. II. Zooplankton, primary producers and final conclusions, Aquat. Toxicol. 48 (2000) 251–264.
[5] Y. Yu, X. Chu, G. Pang, Y. Xiang, H. Fang, Effects of repeated applications of fungicide carbendazim on its persistence and microbial community in soil, J. Environ. Sci. 21 (2009) 179–185.
[6] Y. Zhang, H. Wang, X. Wang, B. Hu, C. Zhang, W. Jin, S. Zhu, G. Hu, Q. Hong, Identification of the key amino acid sites of the carbendazim hydrolase (*MheI*) from a novel carbendazim-degrading strain *Mycobacterium* sp. SD-4, J. Hazard. Mater. 331 (2017) 55–62.
[7] IUPAC, Carbendazim. ⟨http://sitem.herts.ac.uk/aeru/iupac/Reports/116.htm⟩. Accessed 15 Jan 2017.
[8] E.P. da Costa, S.E.C. Bottrel, M.C.V.M. Starling, M.M.D. Leão, C.C. Amorim, Degradation of carbendazim in water via photo-Fenton in raceway pond reactor: assessment of acute toxicity and transformation products, Environ. Sci. Pollut. Res. 26 (2019) 4324–4336.
[9] M. Rabiet, C. Margoum, V. Gouy, N. Carluer, M. Coquery, Assessing pesticide concentrations and fluxes in the stream of a small vineyard catchment-effect of sampling frequency, Environ. Pollut. 158 (2010) 737–748.
[10] M. Loewy, V. Kirs, G. Carvajal, A. Venturino, A.M. Pechen de D'Angelo, Groundwater contamination by azinphos methyl in the Northern Patagonic Region (Argentina), Sci. Total Environ. 225 (1999) 211–218.
[11] R. Loos, S. Tavazzi, B. Paracchini, E. Canuti, C. Weissteiner, Analysis of polar organic contaminants in surface water of the northern adriatic sea by solid-phase extraction followed by ultrahigh-pressure liquid chromatography-QTRAP® MS using a hybrid triple-quadrupole linear ion trap instrument, Anal. Bioanal. Chem. 405 (2013) 5875–5885.
[12] M. Burkhart, S. Kupper, P. Hean, R. Schmid, R. Haag, L. Rossi, M. Boller, Release of biocides from urban areas into aquatic systems, Nova Technol. 3 (2007) 1483–1489.
[13] C.C. Montagner, C. Vidal, R.D. Acayaba, W.F. Jardim, I.C.S.F. Jardim, G. A. Umbuzeiro, Trace analysis of pesticides and an assessment of their occurrence in surface and drinking waters from the State of São Paulo (Brazil), Anal. Methods 6 (2014) 6668–6677.
[14] V. Rizzi, J. Gubitosa, P. Fini, R. Romita, A. Agostiano, S. Nuzzo, P. Cosma, Commercial bentonite clay as low-cost and recyclable "natural" adsorbent for the Carbendazim removal/recover from water: overview on the adsorption process and preliminary photodegradation considerations, Colloid Surf. A 602 (2020), 125060.
[15] V.P. Salunkhe, I.S. Sawant, K. Banerjee, P.N. Wadkar, S.D. Sawant, S.A. Hingmire, Kinetics of degradation of carbendazim by B. subtilis strains: possibility of in situ detoxification, Environ. Monit. Assess. 186 (2014) 8599–8610.
[16] J. Saien, S. Khezrianjoo, Degradation of the fungicide carbendazim in aqueous solutions with UV/TiO_2 process: optimization, kinetics and toxicity studies, J. Hazard. Mater. 157 (2008) 269–276.
[17] M. Li, Z. Zhang, Z. Li, H. Wu, Removal of nitrogen and phosphorus pollutants from water by $FeCl_3$- impregnated biochar, Ecol. Eng. 149 (2020), 105792.

[18] Y. Dai, N. Zhang, C. Xing, Q. Cui, Q. Sun, The adsorption, regeneration and engineering applications of biochar for removal organic pollutants: a review, Chemosphere 223 (2019) 12–27.
[19] N. You, J.Y. Li, H.T. Fa, H. Shen, In-situ sampling of nitrophenols in industrial wastewaters using diffusive gradients in thin films based on lignocellulose-derived activated carbons, J. Adv. Res. 15 (2019) 77–86.
[20] Y.G. Lee, J. Shin, J. Kwak, S. Kim, C. Son, G.Y. Kim, C.H. Lee, K. Chon, Enhanced adsorption capacities of fungicides using peanut shell biochar via successive chemical modification with $KMnO_4$ and KOH, Separations 8 (2021) 52.
[21] S. Li, T. You, Y. Guo, S. Yao, S. Zang, M. Xiao, Z. Zhang, Y. Shen, High dispersions of nano zero valent iron supported on biochar by one-step carbothermal synthesis and its application in chromate removal, RSC Adv. 9 (2019) 12428–12435.
[22] C. Liu, W. Wang, R. Wu, Y. Liu, X. Lin, H. Kan, Y. Zheng, Preparation of acid- and alkali-modified biochar for removal of methylene blue pigment, ACS Omega 5 (2020) 30906–30922.
[23] F. Suo, X. You, Y. Ma, Y. Li, Rapid removal of triazine pesticides by P doped biochar and the adsorption mechanism, Chemosphere 235 (2019) 918–925.
[24] N. You, Y. Chen, Q.X. Zhang, Ying Zhang, Z. Meng, H.T. Fan, *In-situ* monitoring of phenol in surface waters by diffusive gradients in thin films technique based on the nanocomposites of zero-valent iron@biochar, Sci. Total. Environ. 735 (2020), 139553.
[25] C. Wan, H. Li, L. Zhao, Z. Li, C. Zhang, X. Tan, X. Liu, Mechanism of removal and degradation characteristics of dicamba by biochar prepared from Fe-modified sludge, J. Environ. Manag. 299 (2021), 113602.
[26] T. Ding, T. Huang, Z. Wu, W. Li, K. Guo, J. Li, Adsorption-desorption behavior of carbendazim by sewage sludge-derived biochar and its possible mechanism, RSC Adv. 9 (2019) 35209–35216.
[27] T. Wang, Z. Zhang, H. Zhang, X. Zhong, Y. Liu, S. Liao, X. Yue, G. Zhou, Sorption of carbendazim on activated carbons derived from rape straw and its mechanism, RSC Adv. 9 (2019) 41745–41754.
[28] P. Peng, Y.H. Lang, X.M. Wang, Adsorption behavior and mechanism of pentachlorophenol on reed biochars: pH effect, pyrolysis temperature, hydrochloric acid treatment and isotherms, Ecol. Eng. 90 (2016) 225–233.
[29] D.W. Cho, K. Yoon, E.E. Kwon, J.K. Biswas, H. Song, Fabrication of magnetic biochar as a treatment medium for As(V) via pyrolysis of $FeCl_3$-pretreated spent coffee ground, Environ. Pollut. 229 (2017) 942–949.
[30] R. Zhao, X. Ma, J. Xu, Q. Zhang, Removal of the pesticide imidacloprid from aqueous solution by biochar derived from peanut shell, BioResources 13 (2) (2018) 5656–5669.
[31] B. Chen, D. Zhou, L. Zhu, Transitional adsorption and partition of nonpolar and polar aromatic contaminants by biochars of pine needles with different pyrolytic temperatures, Environ. Sci. Technol. 42 (2008) 5137–5143.
[32] M. Keiluweit, P.S. Nico, M.G. Johnson, M. Kleber, Dynamic molecular structure of plant biomass-derived black carbon (biochar), Environ. Sci. Technol. 44 (2010) 1247–1253.
[33] A.F. Martins, Ad.L. Cardoso, J.A. Stahl, J. Diniz, Low temperature conversion of rice husks, eucalyptus sawdust and peach stones for the production of carbon-like adsorbent, Bioresour. Technol. 98 (2007) 5–1100.
[34] W.J. Liu, K. Tian, H. Jiang, H.Q. Yu, Facile synthesis of highly efficient and recyclable magnetic solid acid from biomass waste, Sci. Rep. 3 (2013) 2419.
[35] X.Y. Zhou, F. Xie, M. Jiang, K.A. Li, S.G. Tian, Physicochemical properties and lead ion adsorption of biochar prepared from Turkish gall residue at different pyrolysis temperatures, Microsc. Res. Tech. 84 (2021) 1003–1011.
[36] T. Bera, T.J. Purakayastha, A.K. Patra, S.C. Datta, Comparative analysis of physicochemical, nutrient, and spectral properties of agricultural residue biochars as influenced by pyrolysis temperatures, J. Mater. Cycles Waste 20 (2018) 1115–1127.
[37] D. Mohan, H. Kumar, A. Sarswat, M. Alexandre-Franco, C.U. Pittman, Cadmium and lead remediation using magnetic oak wood and oak bark fast pyrolysis biochars, Chem. Eng. J. 236 (2014) 513–528.
[38] M. Rafiq, R. Bachmann, M. Rafiq, Z. Shang, S. Joseph, R. Long, Influence of pyrolysis temperature on physico-chemical properties of corn stover (*Zea mays* L.) biochar and feasibility for carbon capture and energy balance, PLoS One 11 (6) (2016), e0156894.
[39] P. Zhang, H. Sun, L. Yu, T. Sun, Adsorption and catalytic hydrolysis of carbaryl and atrazine on pig manure-derived biochars: impact of structural properties of biochars, J. Hazard. Mater. 244–245 (2013) 217–224.
[40] X. Xi, A.J. Yan, G. Quan, L. Cui, Removal of the pesticide pymetrozine from aqueous solution by biochar produced from Brewer's spent grain at different pyrolytic temperatures, BioResources 9 (4) (2014) 7696–7709.
[41] M.Y. Khan, A.S. Mangrich, J. Schultz, F.S. Grasel, N. Mattoso, D.H. Mosca, Green chemistry preparation of superparamagnetic nanoparticles containing Fe_3O_4 cores in biochar, J. Anal. Appl. Pyrolysis 116 (2015) 2–48.
[42] B. Chen, Z. Chen, S. Lv, A novel magnetic biochar efficiently sorbs organic pollutants and phosphate, Bioresour. Technol. 102 (2011) 716–723.
[43] N. Liu, A.B. Charrua, C.H. Weng, X. Yuan, F. Ding, Characterization of biochars derived from agriculture wastes and their adsorptive removal of atrazine from aqueous solution: a comparative study, Bioresour. Technol. 198 (2015) 55–62.
[44] S. Chen, C. Qin, T. Wang, F. Chen, X. Li, H. Hou, M. Zhou, Study on the adsorption of dyestuffs with different properties by sludge-rice husk biochar: adsorption capacity, isotherm, kinetic, thermodynamics and mechanism, J. Mol. Liq. 285 (2019) 62–74.
[45] Z. Feng, N. Chen, C. Feng, Y. Gao, Mechanisms of Cr(VI) removal by $FeCl_3$-modified lotus stem-based biochar ($FeCl_3$@LS-BC) using mass-balance and functional group expressions, Colloid Surf. A 551 (2018) 17–24.
[46] M. Rajabi, B. Mirza, K. Mahanpoor, M. Mirjalili, F. Najafi, O. Moradi, H. Sadegh, R. Shahryari-ghoshekandi, M. Asif, I. Tyagi, S. Agarwal, V.K. Gupta, Adsorption of malachite green from aqueous solution by carboxylate group functionalized multi-walled carbon nanotubes: determination of equilibrium and kinetics parameters, J. Ind. Eng. Chem. 34 (2016) 130–138.
[47] M.Z. Afzal, X.F. Sun, J. Liu, C. Song, S.G. Wang, A. Javed, Enhancement of ciprofloxacin sorption on chitosan/biochar hydrogel beads, Sci. Total Environ. 639 (2018) 560–569.
[48] Z. Liu, F.S. Zhang, Removal of lead from water using biochars prepared from hydrothermal liquefaction of biomass, J. Hazard. Mater. 167 (2009) 933–939.
[49] Y.X. Song, S. Chen, N. You, H.T. Fan, L.N. Sun, Nanocomposites of zero-valent iron@activated carbon derived from corn stalk for adsorptive removal of tetracycline antibiotics, Chemosphere 255 (2020), 126917.
[50] H.T. Fan, L.Q. Shi, H. Shen, X. Chen, K. Xie, Equilibrium, isotherm, kinetic and thermodynamic studies for removal of tetracycline antibiotics by adsorption onto hazelnut shell derived activated carbons from aqueous media, RSC Adv. 6 (2016) 109983–109991.
[51] L. Yan, Y. Liu, Y. Zhang, S. Liu, C. Wang, W. Chen, C. Liu, Z. Chen, Y. Zhang, $ZnCl_2$ modified biochar derived from aerobic granular sludge for developed microporosity and enhanced adsorption to tetracycline, Bioresour. Technol. 297 (2020), 122381.
[52] Z. Zeng, S. Ye, H. Wu, R. Xiao, G. Zeng, J. Liang, C. Zhang, J. Yu, Y. Fang, B. Song, Research on the sustainable efficacy of g-MoS_2 decorated biochar nanocomposites for removing tetracycline hydrochloride from antibiotic-polluted aqueous solution, Sci. Total Environ. 648 (2019) 206–217.
[53] D. Hao, Y. Chen, Y. Zhang, Nan You, Nanocomposites of zero-valent iron@biochar derived from agricultural wastes for adsorptive removal of tetracyclines, Chemosphere 284 (2021), 131342.
[54] N. Ni, T. Sanghvi, S.H. Yalkowsky, Solubilization and preformulation of carbendazim, Int. J. Pharm. 244 (2002) 99–104.
[55] Y. Ma, Y. Qi, L. Yang, L. Wu, P. Li, F. Gao, X. Qi, Z. Zhang, Adsorptive removal of imidacloprid by potassium hydroxide activated magnetic sugarcane bagasse biochar: adsorption efficiency, mechanism and regeneration, J. Clean. Prod. 292 (2021), 126005.
[56] S. Fan, J. Tang, Y. Wang, H. Li, H. Zhang, J. Tang, Z. Wan, X. Li, Biochar prepared from co-pyrolysis of municipal sewage sludge and tea waste for the adsorption of methylene blue from aqueous solutions: Kinetics, isotherm, thermodynamic and mechanism, J. Mol. Liq. 220 (2016) 432–441.
[57] Y. Li, S. Wang, Y. Zhang, R. Han, W. Wei, Enhanced tetracycline adsorption onto hydroxyapatite by Fe(III) incorporation, J. Mol. Liq. 247 (2017) 171–181.